LA-UR- 08-5221

Approved for public release; distribution is unlimited.

Title:	Nanoscale Growth Twins in Sputtered Metal Films
Author(s):	Amit Misra, LANL; Osman Anderoglu, LANL; Richard Hoagland, LANL; X. Zhang, Texas A&M.
Intended for:	Journal: JOM - A publication of the Minerals, Metals and Materials Society

Los Alamos
NATIONAL LABORATORY
EST. 1943

Los Alamos National Laboratory, an affirmative action/equal opportunity employer, is operated by the Los Alamos National Security, LLC for the National Nuclear Security Administration of the U.S. Department of Energy under contract DE-AC52-06NA25396. By acceptance of this article, the publisher recognizes that the U.S. Government retains a nonexclusive, royalty-free license to publish or reproduce the published form of this contribution, or to allow others to do so, for U.S. Government purposes. Los Alamos National Laboratory requests that the publisher identify this article as work performed under the auspices of the U.S. Department of Energy. Los Alamos National Laboratory strongly supports academic freedom and a researcher's right to publish; as an institution, however, the Laboratory does not endorse the viewpoint of a publication or guarantee its technical correctness.

Form 836 (7/06)

Nanoscale Growth Twins in Sputtered Metal films

X. Zhang* and O. Anderoglu,

Texas A&M University,

R. G. Hoagland and A. Misra,

Los Alamos National Laboratory, Los Alamos, NM 87545, USA

zhangx@tamu.edu

Abstract

We review recent studies on the mechanical properties of sputtered Cu and 330 stainless steel films with {111} nanoscale growth twins preferentially oriented perpendicular to growth direction. The mechanisms of formation of growth twins during sputtering and the deformation mechanisms that enable usually high strengths in nanotwinned structures are highlighted. Growth twins in sputtered films possess good thermal stability at elevated temperature, providing an approach to extend the application of high strength nanostructured metals to higher temperatures.

1. The observation of nanoscale growth twins in fcc Cu and 330 stainless steel films and their influence on mechanical strength

Twin interface, a low energy planar defect, can be categorized into deformation twins, annealing twins and growth twins. Although each type of twins, especially deformation twins, has been studied extensively in the past, the influence of nanoscale high density twins on mechanical properties have drawn a renewed interest recently. Deformation twins have been observed in nanocrystalline metals (see article by YT Zhu *et al.* in this issue). Nanoscale growth twins have been recently reported in electrodeposited [1 - 5] and sputter deposited fcc metals [6 - 10], and the latter form the focus of this article.

A high density of growth twins has been observed in sputtered 330 stainless steel (330 SS) and Cu films recently [6,7]. As shown in Fig. 1a and 1b, twin interfaces in both cases are of {111} type, oriented perpendicular to growth direction. The average twin lamellae thickness in both cases is less than 10 nm. The hardness of nanotwinned 330 SS and Cu films is approximately 6.5 and 3.5 GPa, respectively, much higher than their bulk counterparts. Sputtered thick Cu foils possess 1-2% uniform elongation with a tensile strength of 1.2 GPa [7]. These high density growth twins pose significant resistance to the transmission of dislocations. As shown in Fig. 2 by molecular dynamics simulations of twin interface in fcc Ni, in the event of applying a pure shear stress, Fig. 2b, a resolved shear stress, ~ 1.7 GPa, is necessary to transmit the glide dislocation across the twin interface onto the complementary {111} glide plane, leaving behind a large magnitude of residual Burgers vector at the twin boundary [6]. In a different simulation (Fig. 2c), the slip transmission was studied under applied tension. Here, given the direction of the applied tension and the sign of the Burgers vector of the dislocation gliding towards the twin boundary, there is no net force to produce a glide dislocation that moves away from the boundary

on the complementary {111} twin plane. Hence, slip is observed to transmit onto {200}plane, a non typical glide plane in fcc, at a resolved shear stress of ~ 3 GPa [9]. MD simulations thus indicate that the inherent strength of the twin interface to the transmission of single dislocations is rather high. A single dislocation was considered in the simulation since a dislocation pile-up is less likely at twin lamellae thickness of 10 nm or less. The simulations shown in Fig. 2 compute an upper bound estimate of the barrier strength of twin boundaries to slip transmission in the absence of dislocation pile-ups.

The dependence of the strength of nanotwinned metals on the average twin lamellae thickness is discussed in a later section. Tailoring twin spacing in nanotwinned metals is still a scientific challenge in spite of numerous attempts. Understanding the formation mechanisms of growth twins is a key to achieving a wide range of twin spacing in a reproducible way, as discussed in the next section.

2. The formation mechanisms of growth twins in vapor-deposited metals

During physical vapor deposition, atoms from the vapor phase condense on a substrate to form the solid film. The initial nuclei that form may be either 'perfect' (i.e., free of planar defects) or have stacking faults and/or twins. The total free energy (ΔG_1) of a disc-shaped 'perfect' nucleus with radius r and height h is given as:

$$\Delta G_1 = 2\pi rh\gamma - \pi r^2 h\Delta G_v \quad (1)$$

where γ is the surface energy and ΔG_v is the bulk free energy per unit volume driving the nucleation. For the nucleus with a twin interface, eq. (1) is modified to:

$$\Delta G_2 = 2\pi rh\gamma - \pi r^2 h\Delta G_v + \pi r^2 \gamma_t \quad (2)$$

where γ_t is the twin boundary energy. For gas-solid transformation (sputtering in this case), the critical nucleus size r* for the perfect and twin nucleus is [11]

$$r^*_{perfect} = \frac{\gamma}{\left(\frac{kT}{\Omega}\ln\left[\frac{J\sqrt{2\pi mkT}}{P_s}\right]\right)} \quad (3)$$

and

$$r^*_{twin} = \frac{\gamma}{\left(\frac{kT}{\Omega}\ln\left[\frac{J\sqrt{2\pi mkT}}{P_s}\right] - \frac{\gamma_t}{h}\right)}, \text{ respectively} \quad (4)$$

where k is the Boltzmann constant, T is the substrate temperature during deposition, Ω is the atomic volume, J is the deposition flux, and P_s is the vapor pressure above solid. In comparing eq. (3) with (4), we note that $r^*_{perfect} < r^*_{twin}$, and nucleation of a perfect nucleus will be preferred to a twinned nucleus. However, if γ_t is very low and J is very high, then the difference between $r^*_{perfect}$ and r^*_{twin} will be negligibly small, and the formation of twinned nuclei may occur with very high probability during growth.

A series of experiments have been performed to test the predictions of these equations. 330 SS films were deposited at varying rates from 0.5 to 7.5 Å/sec. The volume fraction of twinned grains in 330 SS is very small at low deposition rate, and increases rapidly after deposition rate approaches ~2 Å/sec, and increases moderately thereafter till 50% at a deposition rate of 7.5 Å/sec [12]. On the other hand, the average columnar grain sizes stay roughly constant, ~ 25 nm. These results agree qualitatively with the prediction that ~ 2 Å/sec is necessary, as shown in Fig. 3a, to reduce the difference in radius between twin and perfect nuclei to ~ 10%, and thus promoting the nucleation of twins. In Fig. 3a, $\Delta r/r$ represents $(r^*_{twin} - r^*_{perfect})/r^*_{perfect}$. It is

worthwhile to point out that the average twin spacing in these films remains approximately unchanged, a few nm, i.e. independent of deposition rate in the current deposition conditions in 330 SS. This is likely due to the fact that stainless steel has complicated chemistry, with Fe, Cr and Ni etc. in the composition, and chemistry should play an important role in the formation of growth twins. Such aspect can not be captured by the thermodynamics model where only stacking fault energy and certain deposition parameters are considered. The 330 SS film hardness seems to increase monotonically with increasing volume fraction of twinned grains, and approaches 6.5 GPa for films with approximately 50% twinned grains. Zhou and Wadley [13] have modeled the formation of growth twins in Cu during physical vapor deposition using molecular dynamic simulations. Their simulation has shown that the influence of deposition rate and temperature on the formation of growth twins is less significant at a deposition rate of 400 Å/sec or higher, consistent with our calculations that shows at 400 Å/sec or higher, the $\Delta r/r$ value at the tail of the plot varies slightly with deposition rate, and will potentially have little influence on the formation of growth twins. The hardness plot is fitted linearly by the dash line, in Fig. 3b, which intercepts with Y axis at 4.2 GPa. As the volume fraction of growth twins is zero at Y axis, the intercept indicates a lower bound hardness of 330 SS films due primarily to grain boundary induced strengthening, with an average columnar grain size of ~ 25 nm. For materials with relatively higher γ_t (as compared to austenitic SS), such as Ni (43 mJ/m^2 [14]), sputtering at very high deposition rate is needed to form high twin densities [15]. For Al films with a γ_t of 75 mJ/m^2 [14], however, even at a deposition rate of a few nm/s, it is still unlikely to show any stacking faults or twins. The above analysis does not include the film growth stresses that may also influence the formation (e.g., as a strain relief mechanism) of the observed nanoscale

twinning. A recent study shows that the formation of growth twins in 330 SS films depends very little on the sign and magnitude of residual growth stress [9].

3. Thermal stability of twin interface

Although both twin interface and grain boundaries are effective in strengthening metals, twin interface may have certain advantages, such as better thermal stability at elevated temperature. A recent study on thermal stability of nanotwins in sputtered Cu films support this hypothesis [10]. A series of high vacuum annealing experiments were performed on free standing sputtered Cu foils. Annealing up to 800 °C leads to grain coarsening, but the high density of growth twins is retained, as shown in Fig. 4a and b. After annealing at 800 °C, the average columnar grain size increased by an order of magnitude to over 500 nm, whereas the twin lamellae thickness increased only moderately and remained less than 20 nm.

A microstructure comprised of twin boundaries has better thermal stability than high angle grain boundaries because of its low energy characteristics. The energy of a high angle grain boundary in Cu is typically 625-710 mJ/m^2, [14, 16] whereas the twin boundary energy of Cu is much smaller, typically 24-39 mJ/m^2 [14, 17]. Assuming a surface area of 1 m^2, the total grain boundary energy stored within 1 μm thick films shown in Fig. 1b is around 27 J, whereas the total twin boundary energy stored is approximately 5 J. The driving force for reducing the total energy of the system via grain coarsening is higher than that of twin coarsening. After annealing at 800 °C, the total energy stored at column grain boundaries, with an average diameter of 500 nm, is approximately 2.5 J, similar to the energy stored in twin boundaries, 1.25 J, with an average twin spacing of ~ 20 nm. The activation energy for twin boundary migration during coarsening is estimate to be ~ 238 kJ/mol [10], a factor of three higher than the activation energy (83 kJ/mol) for high-angle grain boundary migration in pure Cu [18]. The thermal stability of

columnar grains in nanotwinned Cu seems to be better than nanocrystalline equiaxed grains. Besides the fact that accumulative grain boundary energy in columnar grain boundaries is lower than that in equiaxed grains of the same diameter, ~ 40 nm, faceted columnar grain boundaries observed in annealed nanotwinned Cu may indicate a pinning effect on the migration of grain boundaries. Also Fe precipitates at the grain boundaries (~ 0.5at% Fe in deposited Cu films) may exert a Zener drag force on the high-angle grain boundary migration. MD simulation shows that presence of 1 % Fe in Cu could cause an order of magnitude increase in barrier strength for grain boundary migration [19].

During annealing, the hardness of as deposited Cu thin films decreased gradually and continuously from ~ 3.5 GPa to approximately 2.2 GPa at 800°C as shown in Fig. 5a. In comparison, hardness of nanocrystalline or ultrafine grain (ufg) Cu decreases rapidly to ~ 1 GPa or lower at annealing temperatures of 400 °C [20-22]. A Hall-Petch plot of flow stress vs. $t^{-1/2}$ (where t stands for the average lamella thickness) is given in Fig. 5b for nanotwinned Cu and annealed coarse-grain Cu [23]. The Hall-Petch slope (k) of the bulk Cu is approximately 0.15 $MPa.m^{1/2}$ [23] and its extrapolation to the nanometer range overestimates the peak strength of nanotwinned Cu. A linear fit of the data for nanotwinned Cu gives a slope of ~ 0.06 $MPa.m^{1/2}$, almost a factor of three lower than the k for bulk Cu, indicating that a weaker dependence of flow stress on lamella thickness in twinned Cu.

4. Summary

Vapor-deposition of low stacking fault energy fcc metals produces a nanotwinned structure such that the average twin lamellae thickness is below 10 nm and twin boundaries are preferentially aligned normal to the growth direction. These nanotwinned structures exhibit

unusually high strengths, e.g., tensile strength ≈ 1.2 GPa for Cu and hardness of ≈ 7 GPa for austenitic stainless steels. In the absence of dislocation pile-ups, twin boundaries are strong obstacles for slip transmission. Due to the low energy of a twin boundary as compared to a high-angle grain boundary, the nanotwinned structures exhibit very high thermal stability and much better retention of strength after annealing, as compared to nanocrystalline metals.

With regard to future work, a model that considers chemistry and bonding of materials is needed to understand the formation mechanisms of twin interface in low stacking fault energy metals. Such model will provide insight into the atomic arrangement during twin growth and is likely to shine light for experimental studies. In parallel, extensive experiments are needed to investigate parameters that will tailor twin spacing in a wider range.

Acknowledgement

XZ acknowledges financial support by NSF-DMR under grant no. 0644835. XZ also acknowledges support by the Center for Integrated Nanotechnologies at Los Alamos National Laboratory through user program. AM acknowledges support from DOE, Office of Basic Energy Sciences. Discussions with J. D. Embury, F. Spaepen and J.P. Hirth are also acknowledged.

Reference:

1. L. Lu, Y. Shen, X. Chen, L. Qian, K. Lu. Science, **304** (2004) 422.

2. Luhua Xu,_Pradeep Dixit, Jianmin Miao, John H. L. Pang, Xi Zhang, Robert Preisser and K. N. Tu, Appl. Phys. Lett., **90** (2007) 033111.

3. B.Z. Cui, K. Han, Y. Xin, D.R. Waryoba, A.L. Mbaruku, Acta Mater. **55** (2007) 4429.

4. B.Y.C. Wu, P.J. Ferreira, and C.A. Schuh, Metall. Mater. Trans. A, **36A** (2005) 1927.

5. G. Lucadamo, D. L. Medlin, , N. Y. C. Yang, J. J. Kelly, and A. A. Talin, Phil. Mag. **85** (2005) 2549.

6. X. Zhang, A. Misra, H. Wang, M. Nastasi, J. D. Embury, T. E. Mitchell, R. G. Hoagland, and J. P. Hirth, Appl. Phys. Lett. **84** (2004) 1096.

7. X. Zhang, H. Wang, X.H. Chen, L. Lu, K. Lu, R.G. Hoagland, A. Misra. Appl. Phys. Lett., **88** (2006) 173116.

8. A.M. Hodgea, Y.M. Wang, T.W. Barbee Jr. Materials Science and Engineering A, **429** (2006) 272.

9. X. Zhang, A. Misra, H. Wang, A. L. Lima, M. F. Hundley, R. G. Hoagland, Journal of Applied Physics, **97** (2005) 094302.

10. O. Anderoglu, A. Misra, H. Wang, and X. Zhang, J. Appl. Phys., **103** (2008) 094322.

11. X. Zhang, A. Misra, H. Wang, T. D. Shen, M. Nastasi, T. E. Mitchell, J. P. Hirth, R.G. Hoagland and J. D. Embury. Acta Mater., **52** (2004) 995.

12. X. Zhang, O. Anderoglu, A. Misra, and H. Wang, J. Appl. Phys., **90** (2007) 153101.

13. X. W. Zhou, H. N. G. Wadley. Acta Mater., **47** (1999) 1063.

14. L. E. Murr, "Interfacial phenomena in metals and alloys", Addison-Wesley, Reading, Mass., 1975.

15. S. D. Dahlgren, W. L. Nicholson, M. D. Merz, W. Bollmann, J. F. Devlin and R. Wang, Thin Solid Films, **40** (1977) 345.

16. Y. K. Huang, A. A. Menovsky, F. R. de Boer. NanoStruc Mat 1993; 2: 587.

17. J.P. Hirth, J. Lothe. Theory of dislocations. (2^{nd} ed.) Melbourne: Krieger; 1992.

18. L. Lu, N. R. Tao, L. B. Wang, B. Z. Ding, K. Lu. J. Appl. Phys. **89** (2000) 6408.

19. L. A. Zepeda-Ruiz, G. H. Gilmer, B. Sadigh, A. Caro, T. Oppelstrup, A. V. Hamza, Appl. Phys. Lett., **87** (2005) 231904.

20. S. Okuda, M. Kobiyama, T. Inami, S. Takamura, Scripta Mater., **44** (2001) 2009.

21. M. Kobiyama, T. Inami and S. Okuda. Scripta Mater., **44** (2001) 1547.

22. H. Jiang, T. Zhu, D. P. Butt, I. V. Alexsandrov, T. C. Lowe. Mater. Sci. and Eng., **A290** (2000) 128.

23. N. Hansen and B. Ralph, Acta Metall., **30** (1982) 441.

Figure Captions

Fig. 1 (a) Cross-sectional HRTEM micrograph showing high density growth twins in 330 SS films with an average twin spacing of a few nm [6]. (b) TEM micrograph of growth twins in Cu films with an average twin spacing of ~ 5nm [7].

Fig. 2. MD simulation showing the strength of symmetric (111) twin interface to block dislocation transmission. (a) A perfect glide dislocation with b = 1/2 [101] resides in the upper layer. Unstrained. (b) The model is subject to stresses such that when the resolved shear stress on the dislocation exceeds 1.77GPa, the dislocation moves away from the twin interface. A Shockley partial with b = 1/6 $[\bar{1}\,\bar{1}\,2]$ remains at the interface. (c) In response to a biaxial stress (in a plane parallel to the interface) that exerts a resolved shear stress of 3 GPa, a dislocation moves away from the interface into the lower grain on a {200} plane, leaving a Shockley at the interface. Note that the Shockley has also moved slightly along the interface plane toward the right side of the model.

Fig. 3. (a) $\Delta r/r$, which is $(r^*_{twin} - r^*_{perfect})/ r^*_{perfect}$, decreases with increasing deposition rate, indicating the formation of growth twins is facilitated at a higher deposition rate. The calculation was done using γ_t (twin boundary energy) of 330 SS and the current experimental conditions. Dashed line indicates that at a deposition rate of 2 Å/sec, where the volume fraction of twinned grains increases significantly, the value of $\Delta r/r$ is approximately 10%. (b) Hardness of 330 SS films increases monotonically with increasing volume fraction of twinned grains. Dash line is a linear fit of the experimental data and it intercept with Y axis (volume fraction of twinned grains = 0) at a hardness of 4.2 GPa.

Fig. 4. Cross-sectional TEM micrographs of annealed Cu films. (a) Annealing at 400 °C leads to an average grain size of ~ 230 nm with little change in the average lamellae thickness. (b) Further annealing at 800 °C increases the average grain sizes to ~ 540 nm. (c) Evolution of twin domains and grain size as a function of annealing temperature. Columnar grain size increases by over an order of magnitude, whereas twin spacing increases moderately and remains less than 20 nm after annealing up to 800°C.

Fig. 5. (a) Hardness as a function of annealing temperature for nanotwinned (nt) Cu comparing to the literature data for UFG and nc Cu. Hardness of nt Cu remains higher than 2 GPa after annealing up to 800°C. (b) Plot of flow stress vs. $t^{-1/2}(d^{-1/2})$ where t and d is average twin lamella thickness and grain size, respectively. The data for bulk Cu (coarse grain) Cu from literature are also included for comparison. The dashed line is the extrapolation of bulk Cu.

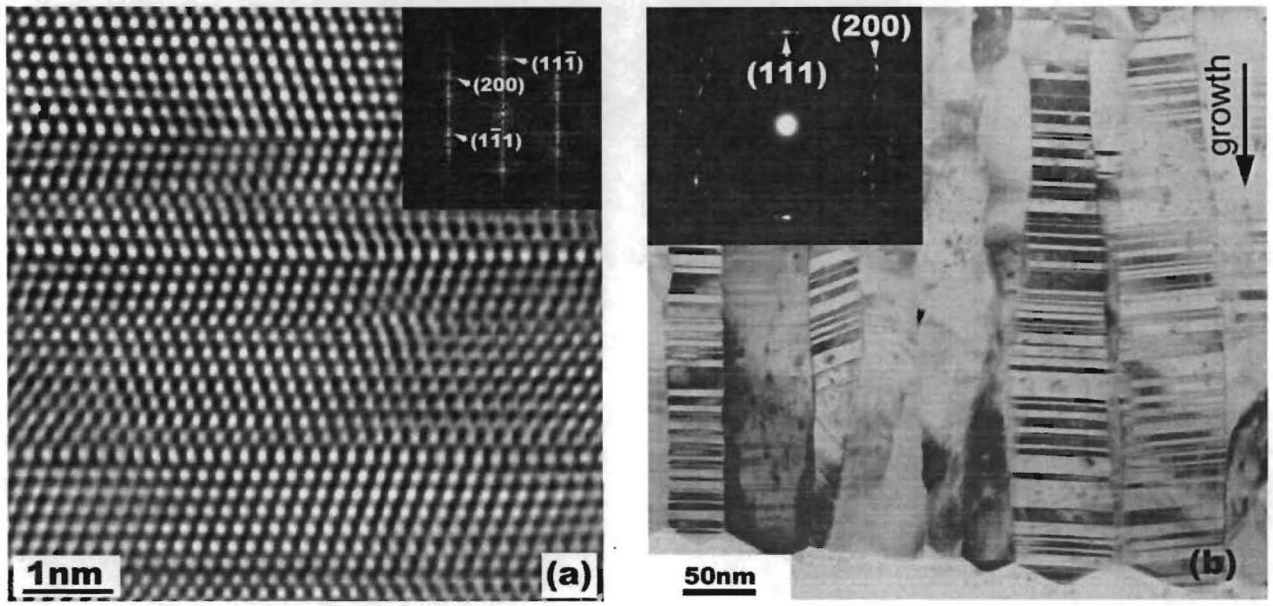

Fig. 1 (a) Cross-sectional HRTEM micrograph showing high density growth twins in 330 SS films with an average twin spacing of a few nm [6]. (b) TEM micrograph of growth twins in Cu films with an average twin spacing of ~ 5nm [7].

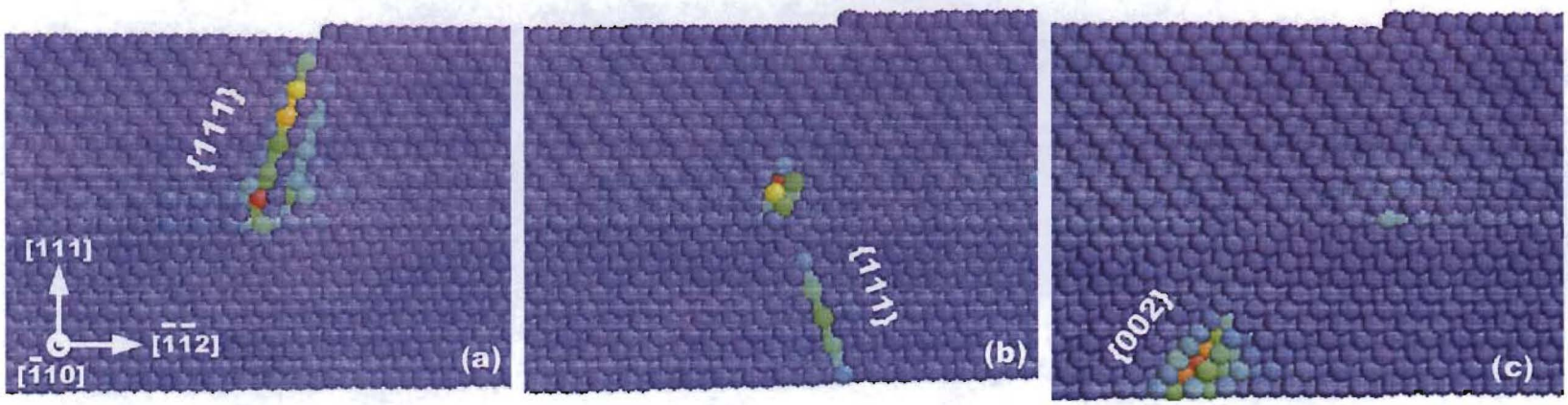

Fig. 2. MD simulation showing the strength of symmetric (111) twin interface to block dislocation transmission. (a) A perfect glide dislocation with b = 1/2 [101] resides in the upper layer. Unstrained. (b) The model is subject to stresses such that when the resolved shear stress on the dislocation exceeds 1.77GPa, the dislocation moves away from the twin interface. A Shockley partial with b = 1/6 [$\bar{1}\bar{1}$2] remains at the interface. (c) In response to a biaxial stress (in a plane parallel to the interface) that exerts a resolved shear stress of 3 GPa, a dislocation moves away from the interface into the lower grain on a {200} plane, leaving a Shockley at the interface. Note that the Shockley has also moved slightly along the interface plane toward the right side of the model.

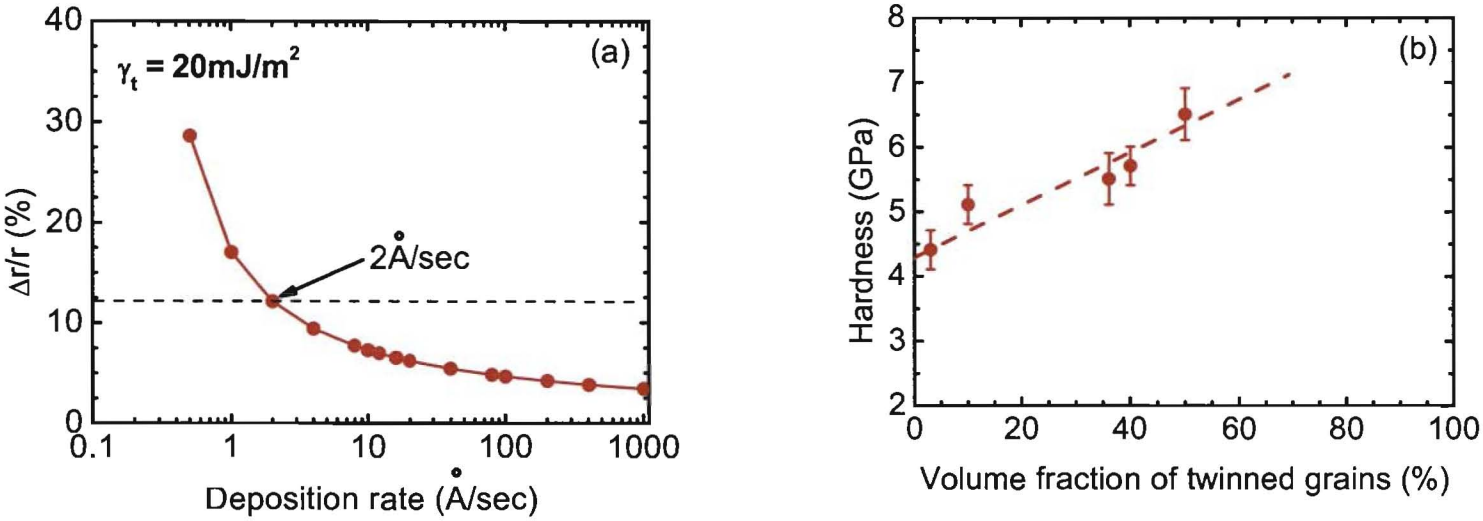

Fig. 3. (a) Δr/r, which is (r^*_{twin} - $r^*_{perfect}$)/ $r^*_{perfect}$, decreases with increasing deposition rate, indicating the formation of growth twins is facilitated at a higher deposition rate. The calculation was done using γ_t (twin boundary energy) of 330 SS and the current experimental conditions. Dashed line indicates that at a deposition rate of 2 Å/sec, where the volume fraction of twinned grains increases significantly, the value of Δr/r is approximately 10%. (b) Hardness of 330 SS films increases monotonically with increasing volume fraction of twinned grains. Dash line is a linear fit of the experimental data and it intercept with Y axis (volume fraction of twinned grains = 0) at a hardness of 4.2 GPa.

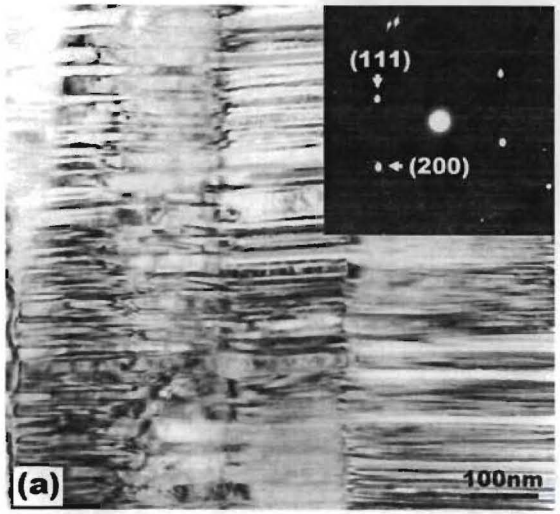

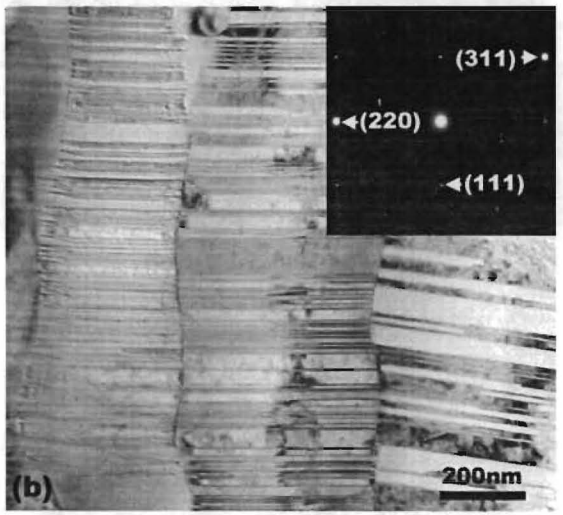

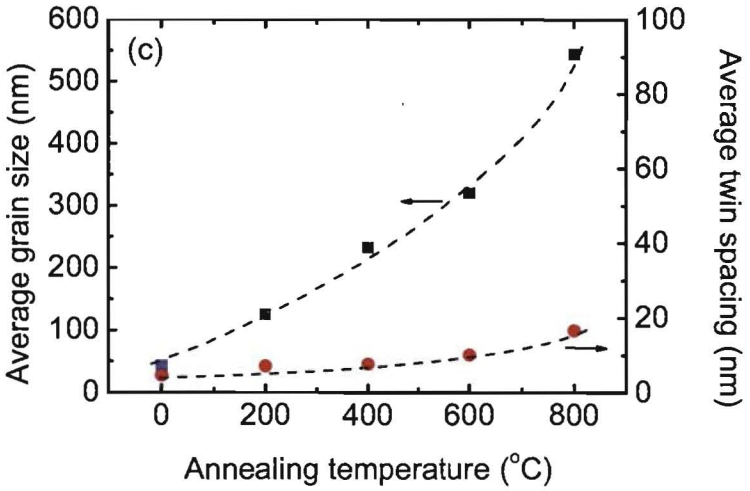

Fig. 4. Cross-sectional TEM micrographs of annealed Cu films. (a) Annealing at 400 °C leads to an average grain size of ~ 230 nm with little change in the average lamellae thickness. (b) Further annealing at 800 °C increases the average grain sizes to ~ 540 nm. (c) Evolution of twin domains and grain size as a function of annealing temperature. Columnar grain size increases by over an order of magnitude, whereas twin spacing increases moderately and remains less than 20 nm after annealing up to 800°C.

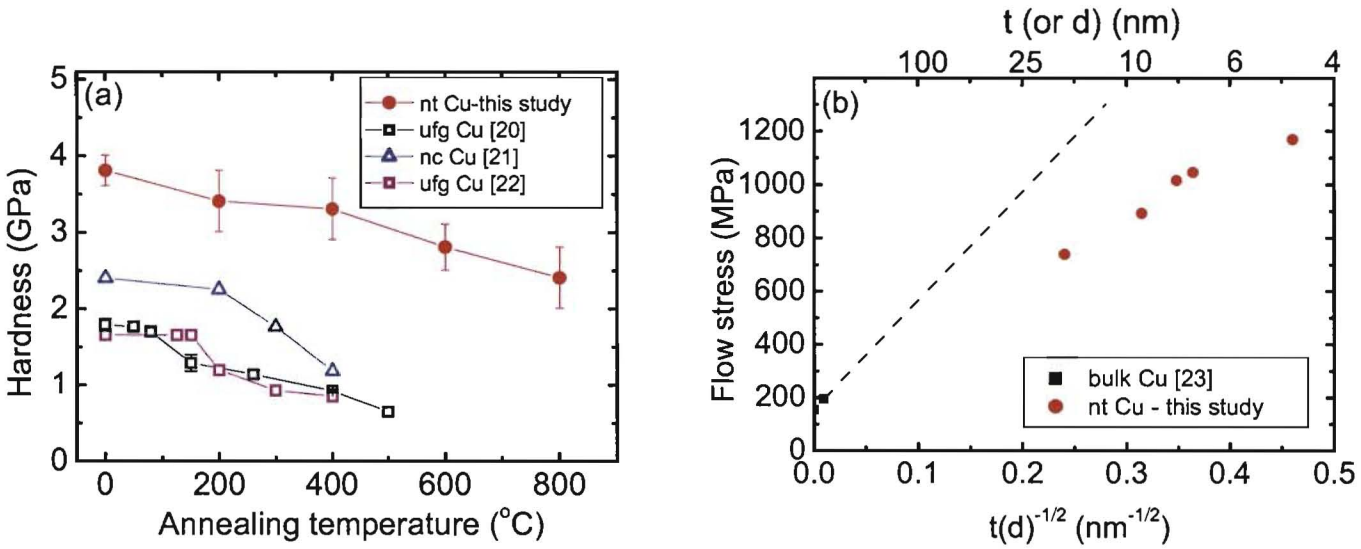

Fig. 5. (a) Hardness as a function of annealing temperature for nanotwinned (nt) Cu comparing to the literature data for UFG and nc Cu. Hardness of nt Cu remains higher than 2 GPa after annealing up to 800°C. (b) Plot of flow stress vs. $t^{-1/2}(d^{-1/2})$ where t and d is average twin lamella thickness and grain size, respectively. The data for bulk Cu (coarse grain) Cu from literature are also included for comparison. The dashed line is the extrapolation of bulk Cu.